

RPPR Final Report
as of 23-Jan-2023

Agency Code: 21XD

Proposal Number: 74854SM

Agreement Number: W911NF-19-2-0089

INVESTIGATOR(S):

Name: Katherine Mirica
Email: katherine.a.mirica@dartmouth.edu
Phone Number: 6036468188
Principal: Y

Organization: **Dartmouth College**

Address: 11 Rope Ferry Rd., Hanover, NH 037551404

Country: USA

DUNS Number: 041027822

EIN: 020222111

Report Date: 28-Nov-2022

Date Received: 29-Nov-2022

Final Report for Period Beginning 01-Mar-2019 and Ending 28-Aug-2022

Title: Stimuli-Responsive Adhesives for Wearable Protection

Begin Performance Period: 01-Mar-2019

End Performance Period: 28-Aug-2022

Report Term: 0-Other

Submitted By: Katherine Mirica

Email: katherine.a.mirica@dartmouth.edu

Phone: (603) 646-8188

Distribution Statement: 1-Approved for public release; distribution is unlimited.

STEM Degrees: 2

STEM Participants: 2

Major Goals: please see attached pdf

Accomplishments: please see uploaded file.

Training Opportunities: Name of Participant: Hana J. Yarbrough

Training Activity: Graduate Course "Polymer Synthesis"

Date(s): September 2020-November 2020

Name of Participant: Hana J. Yarbrough

Training Activity: Graduate Course "Functional Nanomaterials"

Date(s): January 2021-March 2021

Name of Participant: Hana J. Yarbrough

Training Activity: Graduate Course "Methods of Materials Characterization"

Date(s): April 2021-June 2021

Name of Participant: Hana J. Yarbrough

Training Activity: Computational Chemistry Collaboration with Professor Wenlin Zhang at Dartmouth

Date: May 2021

Name of Participant: Hana J. Yarbrough

Professional Development: MATLAB Certification Program

Date(s): November 2020-current

Results Dissemination: The work arising from this project has been disseminated through the theses and publications listed in the Products section of the report.

RPPR Final Report
as of 23-Jan-2023

Honors and Awards: The following awards and honors were given to Katherine Mirica during the reporting period:

Karen E. Wetterhahn Memorial Award for Distinguished Creative or Scholarly Achievement (2021)
Gordon Russell 1955 Fellowship, Dartmouth College (2021)
NIH Maximizing Investigators' Research Award (2020)
Camille Dreyfus Teacher Scholar Award (2020)
NSF CAREER Award (2020)
Cottrell Scholar Award (2019)

Protocol Activity Status:

Technology Transfer: Nothing to Report

PARTICIPANTS:

Participant Type: PD/PI

Participant: Katherine A. Mirica

Person Months Worked: 1.00

Project Contribution:

National Academy Member: N

Funding Support:

Participant Type: Graduate Student (research assistant)

Participant: Hana J. Yarbrough

Person Months Worked: 12.00

Project Contribution:

National Academy Member: N

Funding Support:

Participant Type: Graduate Student (research assistant)

Participant: Nicholas Blelloch J.

Person Months Worked: 12.00

Project Contribution:

National Academy Member: N

Funding Support:

ARTICLES:

RPPR Final Report as of 23-Jan-2023

Publication Type: Journal Article Peer Reviewed: Y **Publication Status:** 1-Published

Journal: Chemistry of Materials

Publication Identifier Type: Other

Volume: 32

Issue:

Publication Identifier:

First Page #: 9882

Date Submitted: 8/30/21 12:00AM

Date Published: 11/26/20 10:00AM

Publication Location:

Article Title: Crystal Engineering of Molecular Solids as Temporary Adhesives

Authors: Nicholas D. Blelloch, Haydn T. Mitchell, Carly C. Tymm, Douglas W. Van Citters, and Katherine A. Miric

Keywords: sublimable adhesives, molecular solids, crystal engineering

Abstract: Crystal engineering of temporary adhesion is important in diverse fields ranging from healthcare to manufacturing. Molecular solids—a broad class of crystalline materials characterized by discrete molecules with well-defined chemical and crystal structures—can be utilized as sublimable adhesives to achieve rapid adhesion, strong mechanical bonding, and facile on-demand release of surfaces. Through systematic investigation of the interfacial and bulk properties of molecular solids, this paper shows that this class of materials can exhibit remarkable mechanical strength (resistance to shear stress up to 2100 kPa and shear strain up to 37, as well as shear moduli of up to 1000 kPa), yet enable on-demand (within minutes) release from adhesion through controlled sublimation without the application of solvents and/or mechanical force.

Distribution Statement: 2-Distribution Limited to U.S. Government agencies only; report contains proprietary info
Acknowledged Federal Support: Y

Publication Type: Journal Article Peer Reviewed: Y **Publication Status:** 1-Published

Journal: Crystal Growth and Design

Publication Identifier Type: DOI

Volume:

Issue:

Publication Identifier: 10.1021/acs.cgd.1c00593

First Page #:

Date Submitted: 11/28/22 12:00AM

Date Published:

Publication Location:

Article Title: Photochemical Control of the Mechanical and Adhesive Properties of Crystalline Molecular Solids

Authors: Nicholas D. Blelloch, Haydn T. Mitchell, Louisa C. Greenburg, Douglas W. Van Citters, and Katherine A.

Keywords: molecular solids, adhesives, crystal engineering

Abstract: This paper describes a systematic investigation of the mechanical and adhesive properties of four novel photoresponsive crystalline molecular solids. Each molecular solid comprises a benzyl, naphthyl, or adamantyl scaffold modified with a nitrobenzyl photolabile protecting group. Mechanical and adhesive testing, which recorded shear strengths in the range of 50-150 kPa, provide a direct measurement of the strength of the interfacial intermolecular interactions present within these materials. These interactions were visualized and rationalized using X-ray diffraction techniques and light microscopy. Disruption of interfacial interactions is facilitated by light-induced deprotection of the nitrobenzyl group. Depending on the strategic selection of adhesive, UV irradiation may result in up to a fourfold increase, or a complete elimination in the observed adhesive strength.

Distribution Statement: 4-Distribution authorized to the Department of Defense and U.S. DoD contractors only
Acknowledged Federal Support: Y

RPPR Final Report as of 23-Jan-2023

Publication Type: Journal Article Peer Reviewed: Y **Publication Status:** 1-Published
Journal: Chemical Science
Publication Identifier Type: DOI **Publication Identifier:** 10.1039/D1SC03426J
Volume: **Issue:** **First Page #:**
Date Submitted: 11/28/22 12:00AM **Date Published:**
Publication Location:

Article Title: Stimuli-Responsive Temporary Adhesives: Enabling Debonding On Demand Through Strategic Molecular Design

Authors: Nicholas D. Blelloch, Hana J. Yarbrough, and Katherine A. Mirica

Keywords: adhesives, debonding, stimuli-responsive

Abstract: Stimuli-responsive temporary adhesives constitute a rapidly developing class of materials defined by the modulation of adhesion upon exposure to an external stimulus or stimuli. Engineering these materials to shift between two characteristic properties, strong adhesion and facile debonding, can be achieved through design strategies that target molecular functionalities. In this perspective, we review the recent design and development of these materials, with a focus on the different stimuli that may initiate debonding. These stimuli include UV light, thermal energy, chemical triggers, and other potential triggers such as pressure and mechanical force. We conclude by discussing the fundamental value of systematic investigations into the structure–property relationships within these materials and opportunities for unlocking novel functionalities in future adhesives.

Distribution Statement: 3-Distribution authorized to U.S. Government Agencies and their contractors

Acknowledged Federal Support: Y

DISSERTATIONS:

Publication Type: Thesis or Dissertation

Institution: Dartmouth College

Date Received: 24-Sep-2021

Completion Date: 7/15/21 7:00AM

Title: MOLECULAR DESIGN AND STRUCTURE–PROPERTY RELATIONSHIPS OF STIMULI-RESPONSIVE CRYSTALLINE MATERIALS FOR TEMPORARY ADHESION

Authors: Nicholas Blelloch

Acknowledged Federal Support: Y

Publication Type: Thesis or Dissertation

Institution: Dartmouth College

Date Received: 28-Nov-2022

Completion Date: 11/4/22 2:26AM

Title: Molecular Engineering of Self-Immolative Polymers as Chemically Responsive Temporary Adhesives for Protective Garments

Authors: Hana J. Yarbrough

Acknowledged Federal Support: Y

RPPR Final Report
as of 23-Jan-2023

Partners

Natalie Pomerantz
Natick, MA USA

4

collaboration on adhesive testing and reactivity with simulants

I certify that the information in the report is complete and accurate:

Signature: Katherine Mirica

Signature Date: 11/29/22 2:10PM

Major Goal 1: Design and synthesis of stimuli-responsive adhesives that promote interfacial bonding and on-demand debonding of fabric layers.

1.1 Design and synthesis of stimuli-responsive adhesives capable of chemical response to nerve agent simulants. Progress: 90% complete. A self-immolative polymer with end caps designed to react with fluoride ions was successfully synthesized (up to 3 g scale) and purified (>95% pure). Purity, structure, and thermal properties of the resulting polymeric material was characterized.

1.2 Chemical actuation of the designed adhesives by nerve agents. Progress: 50% complete. Selective depolymerization of a self-immolative polymer with fluoride ions was studied with proton NMR and gel permeation chromatography. Chemical actuation was also studied with fluorescence spectroscopy.

1.3 Design and synthesis of stimuli-responsive adhesives capable of chemical response to mustard agent simulants. Progress: 10% complete. An end cap for a self-immolative polymer was designed to react with a sulfur mustard mimic. COVID restrictions delayed this task due to restructuring of priorities.

1.4 Chemical actuation of the designed adhesives by mustard agents. Progress: 10% complete. An end cap for a self-immolative polymer was designed to react with a sulfur mustard mimic. COVID restrictions delayed this task due to restructuring of priorities.

1.5 Measurement of the rate of reaction of the designed adhesives with target chemicals. Progress: 90% complete. Studies focused on the depolymerization kinetic analysis for two sets of end caps on poly(phthalaldehyde): one set that has no known reactivity and one set that is cleaved with fluoride ions. The influence of acid strength on the depolymerization rate was also studied using benzoic acid and trifluoroacetic acid. Characterization methods include proton NMR, fluorescence spectroscopy, and gel permeation chromatography.

1.6 Assessment of the selectivity and sensitivity of designed adhesives towards target chemicals, and test against common interferents (e.g., sweat). Progress: 90% complete. Poly(phthalaldehyde) exhibited concentration-dependent depolymerization responses to analytes such as fluoride ions and acids, yet remained intact in an aqueous environment.

1.7 Demonstration of bonding of fabrics by designed adhesives, or their rapidly accessible chemical prototypes. Progress: 90% complete. Bonding was assessed on glass and Nyco using solvent-assisted annealing techniques. Subsequent optimization of bonding with the addition of a plasticizer achieved shear strengths of 1000 kPa on glass and 130 kPa on Nyco.

1.8 On-demand delamination of bonded fabrics through sublimation achieved by strategic control of ambient temperature and pressure. Progress: 100% complete. Debonding by sublimation of molecular adhesives has been achieved. The priority of this goal shifted to focus on debonding by stimulus-triggered depolymerization with self-immolative polymers.

Major Goal 2: Assessment and optimization of the chemical and mechanical properties of adhesive/fabric composites in response to CWAs.

2.1 Optimization of stimuli-responsive design for enhancement of the rate of reactivity with nerve agent simulants. Progress: 50% complete. Depolymerization of the fluoride-sensitive polymer was dependent on polymer chain length, where shorter polymers reacted faster than longer chains. Efforts were devoted to optimizing polymer stability.

2.2 Optimization of stimuli-responsive design for enhancement of selectivity towards nerve agent simulants over potential interferents. Progress: 50% complete. Selective depolymerization of the fluoride-sensitive polymer was achieved.

2.3 Measurement of the rate of sublimation of stimuli-responsive adhesives using quartz crystal microbalance. Progress: 0% complete. This task was abandoned due to revised focus of polymeric systems.

2.4 Optimization of stimuli-responsive design for the enhancement of the rate of sublimation or decontamination. Progress: 0% complete. This task was abandoned due to revised focus of polymeric systems.

2.5 Optimization of stimuli-responsive design for enhancement of the rate of reactivity with mustard agent simulants. Progress: 0% complete. COVID restrictions delayed this task due to restructuring of priorities.

2.6 Optimization of stimuli-responsive design for enhancement of selectivity towards mustard agent simulants over potential interferents. Progress: 0% complete. COVID restrictions delayed this task due to restructuring of priorities.

2.7 Measurement of the rate of sublimation of stimuli-responsive adhesives using quartz microbalance. Progress: 0% complete. This task was abandoned due to revised focus of polymeric systems.

2.8 Optimization of stimuli-responsive design for the enhancement of the rate of sublimation or decontamination. Progress: 0% complete. This task was abandoned due to revised focus of polymeric systems.

2.9 Development of bonding strategies for stimuli-responsive adhesives with cotton blends and stretchable fabrics. Progress: 90% complete. Adhesion was achieved by dissolving a self-immolative polymer between surfaces substrates (glass and Nyco). Robust adhesion was achieved by blending the polymer with a plasticizer and melting the blend between surfaces, which exhibited shear strengths of 1000 kPa on glass and 130 kPa on Nyco.

Major Goal 3: Implementation and optimization of the adhesive/fabric design within a protective textile composite.

3.1 Optimization of the deposition of the adhesives onto fabrics using melt bonding, patterning, and printing techniques. Progress: 50% complete. Polymer–plasticizer blends were successfully melted between glass and Nyco substrates without depolymerization.

3.2 Assessment and optimization of the chemical, mechanical, and wearable properties of the adhesive/fabric composites. Progress: 50%. Thermal properties, chemical stability, and adhesive strength of polymer-based materials were characterized.

3.3 Incorporation of optimized stimuli-responsive adhesives into layered textile designs. Progress: 30% complete. Bilayered designs of cotton/cotton and Nyco/Nyco bonded with molecular- and polymer-based materials have been achieved.

3.4 Simplification and optimization of chemical design and synthesis to enable scaleup. Progress: 80% complete. Synthesis and purification of self-immolative polymers was achieved in good yields (50-70%) and high purities (>95% pure).

1) Major Activities:

- a. Molecular design of self-immolative polymer adhesives
- b. Studies on bonding properties of polymeric adhesives on glass and textiles
- c. Studies on release of adherends by stimulus-triggered debonding
- d. Development of self-immolative polymer into a fluorescent sensor

2) Specific Objectives:

- a. Synthesize stimuli-responsive polymeric adhesives in sufficient quantity to study their mechanical properties.
- b. Measurement of shear strength of adhesives on various adherends (e.g., glass, Nyco)
- c. Measurement of reaction rates of adhesives with CWAs utilizing various spectroscopic techniques.
- d. Demonstration of release of bonded adherends via stimulus-controlled depolymerization.

3) Significant Results:

Significant results for the reporting period are summarized in the Figures below.

A self-immolative polymer, poly(phthalaldehyde) (PPA), with reactive end caps was successfully synthesized and characterized following purification (**Figures 1-4**). Early investigations into annealing substrates with these polymeric materials focused on using a solvent bonding method, where the polymer was swollen with solvent between surfaces. Cotton and Nyco substrates bonded with PPA debond after exposure to a strong acid but remain intact after exposure to water (**Figures 14-15**). A plasticizer, dimethyl phthalate (DMP), was blended with PPA in order to improve the internal strength of the adhesive and create a glass transition (**Figure 5-6**). Upon heating the polymer/plasticizer blend between substrates, the assemblies were able to withstand loads up to 160 N on glass slides and 25 N on Nyco with very low adhesive areas ($< 2 \text{ cm}^2$) (**Figure 7**). With optimization of the deposition method and heating set up, the Nyco assemblies may be able to withstand higher loads prior to failure. There is also the opportunity to pattern or print this polymer/plasticizer onto textile substrates.

Before triggering depolymerization of PPA in bonded assemblies, we sought to understand the solution-state reactivity of the polymers with acid and fluoride ions before shifting to chemical warfare agent mimics. We found that depolymerization initiated with a weak acid, benzoic acid ($\text{pK}_a = 4.2$), occurred over numerous days, whereas depolymerization with a strong acid, trifluoroacetic acid ($\text{pK}_a = 0.2$), was complete within 6 hours (**Figures 16 and 18**). When PPA contains a silyl ether end cap, head-to-tail depolymerization can be triggered using fluoride ions. In a PPA sample with a bimodal molecular weight distribution (24% 220 kDa and 76% 2.2 kDa), the shorter polymer chains depolymerized faster than the longer chains (**Figure 17**). This observation may be due to the higher ratio of reactive end caps for short polymer chains. Additionally, we tested the reactivity of PPA with a boronate ester end cap towards hydrogen peroxide (**Figure 19**). With NMR spectroscopy, we observed the cleavage of the boronate ester end cap but no significant depolymerization after exposure to 115 equivalents hydrogen peroxide (**Figure 20**). This may be due to the removal of the end cap not exposing the metastable polymer terminal. Both the acid- and fluoride-triggered depolymerization results suggest that the reactivity of the PPA adhesive may be controlled through polymer chain length and analyte reactivity.

Unexpectedly, we observed fluorescent emission from purified PPA materials, which has not been previously reported (**Figures 21-22**). Following initial photophysical characterization, we hypothesized that the assembly of linear PPA into single chain polymer nanoparticles via noncovalent crosslinking interactions promotes fluorescent emission. We reasoned that depolymerization of PPA may be tracked using fluorescence emission and compared to our previous proton NMR study. We found that depolymerization triggered with trifluoroacetic acid exhibited similar behavior when monitored using NMR and fluorescence spectroscopy (**Figures 18 and 23**). Overall, this surprising discovery suggests that PPA as the potential to be developed into a fluorescent sensor that undergoes an amplified response to chemical stimuli, such as chemical warfare agents or other hazardous species (**Figure 26**).

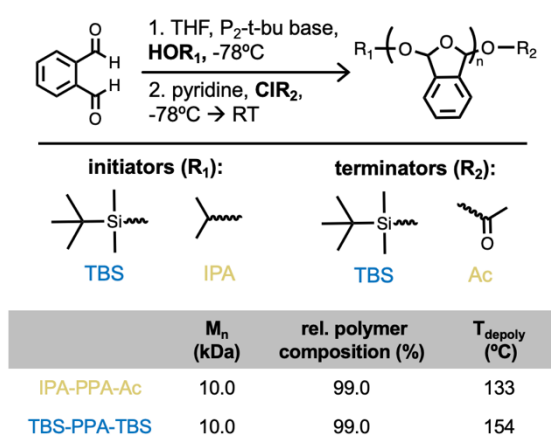


Figure 1. Synthesis and characterization of linear poly(phthalaldehyde) (PPA). Number average molecular weight (M_n) calculated with $^1\text{H-NMR}$. Relative composition calculated from integration of monomer and polymer peaks in $^1\text{H-NMR}$ spectrum. Depolymerization temperature reported as peak temperature from DSC characterization.

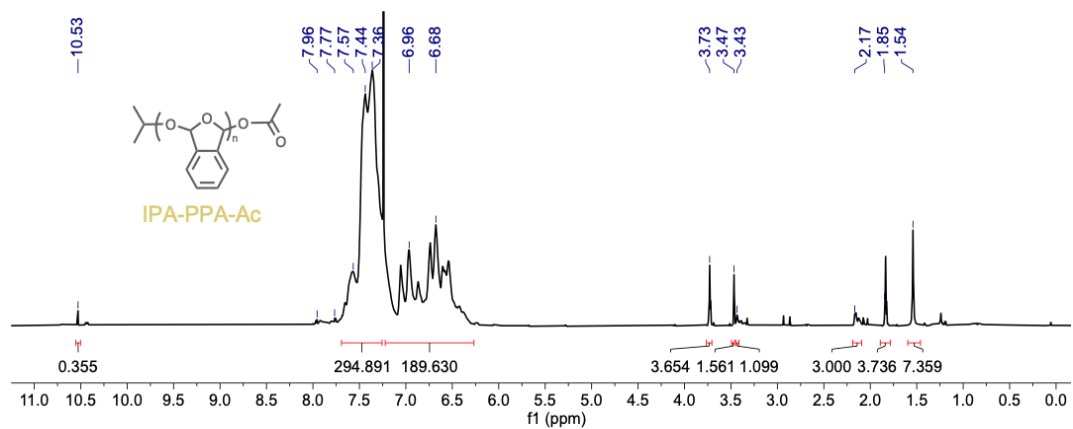


Figure 2. $^1\text{H-NMR}$ spectra (16 scans) of purified IPA-PPA-Ac ($M_n = 10.0$ kDa) in CDCl_3 . Peaks at 10.51, 7.97, and 7.80 ppm represent residual phthalaldehyde monomer.

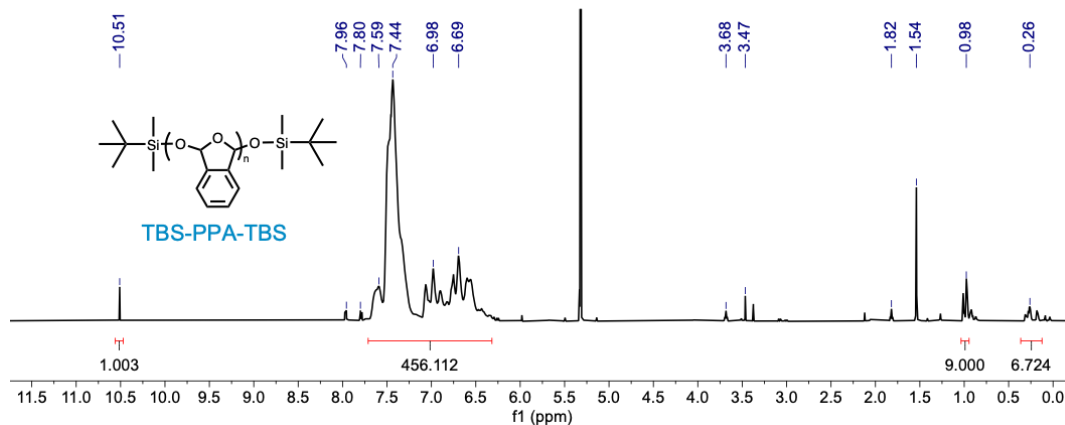


Figure 3. ¹H-NMR spectra (16 scans) of purified TBS-PPA-TBS ($M_n = 10.0$ kDa) in CD₂Cl₂. Peaks at 10.53, 7.96, and 7.77 ppm represent residual phthalaldehyde monomer.

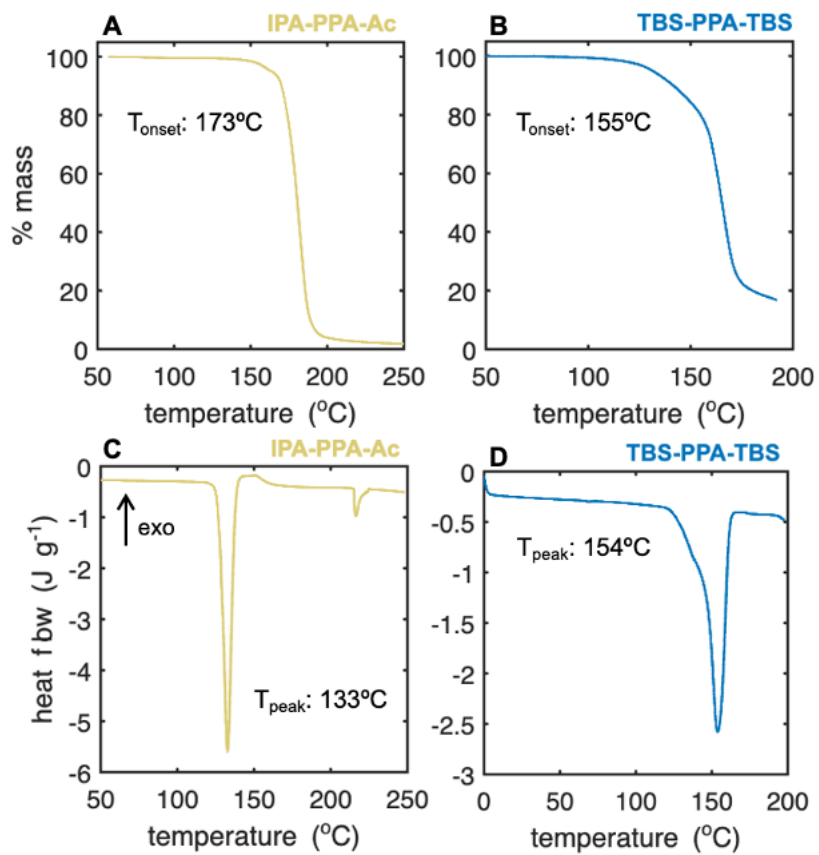


Figure 4. Thermal characterization of IPA-PPA-Ac ($M_n = 10$ kDa, yellow) and TBS-PPA-TBS ($M_n = 10$ kDa, blue). **A)** and **B)** TGA thermograms and **C)** and **D)** DSC thermograms of purified polymeric materials.

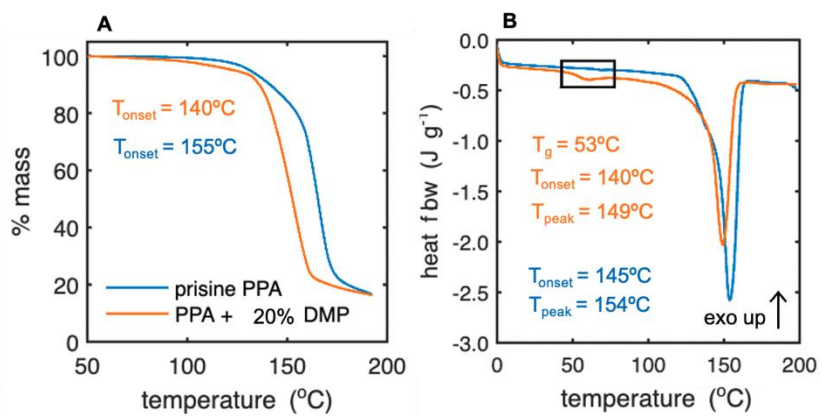


Figure 5. Thermal characterization of TBS-PPA-TBS ($M_n = 10$ kDa) + dimethyl phthalate (DMP). **A)** TGA and **B)** DSC thermogram of pristine TBS-PPA-TBS (blue) and TBS-PPA-TBS + 20% (w/w) DMP (orange).

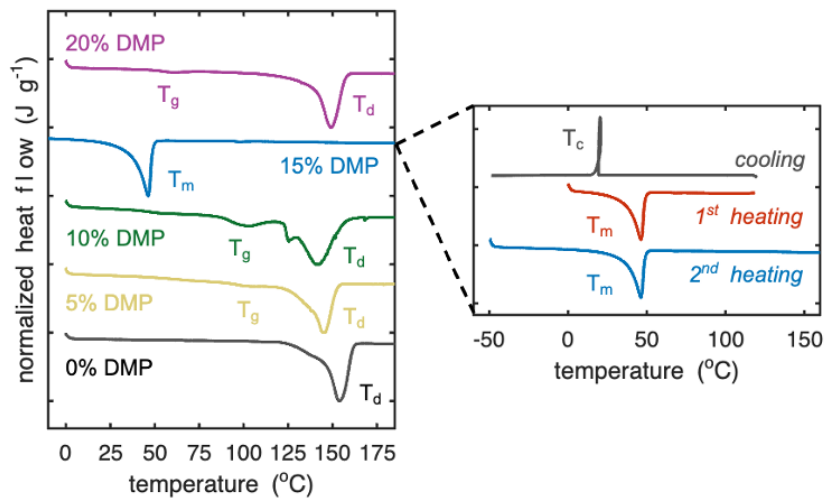


Figure 6. DSC characterization of TBS-PPA-TBS ($M_n = 10$ kDa) with 0-20% (w/w) DMP. Expanded DSC trace for 15% (w/w) DMP sample depicts heating and cooling cycles from 1 measurement. Exo up.

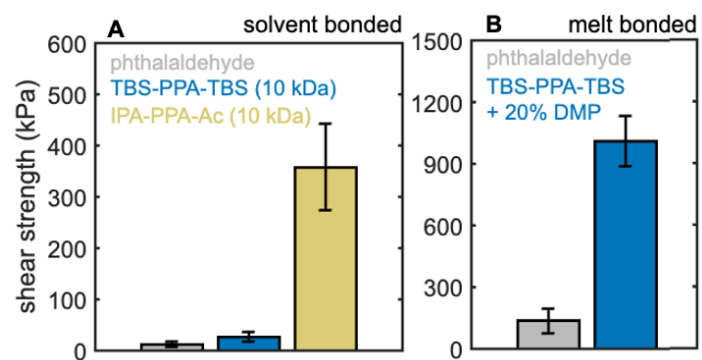


Figure 7. Shear strengths of phthalaldehyde (grey), TBS-PPA-TBS (blue, $M_n = 10$ kDa), and IPA-PPA-Ac (yellow, $M_n = 10$ kDa) assemblies prepared via **A**) solvent (DCM) and **B**) melt bonding methods. Average values calculated with 5-9 replicates. Error bars represent the 95% confidence interval.

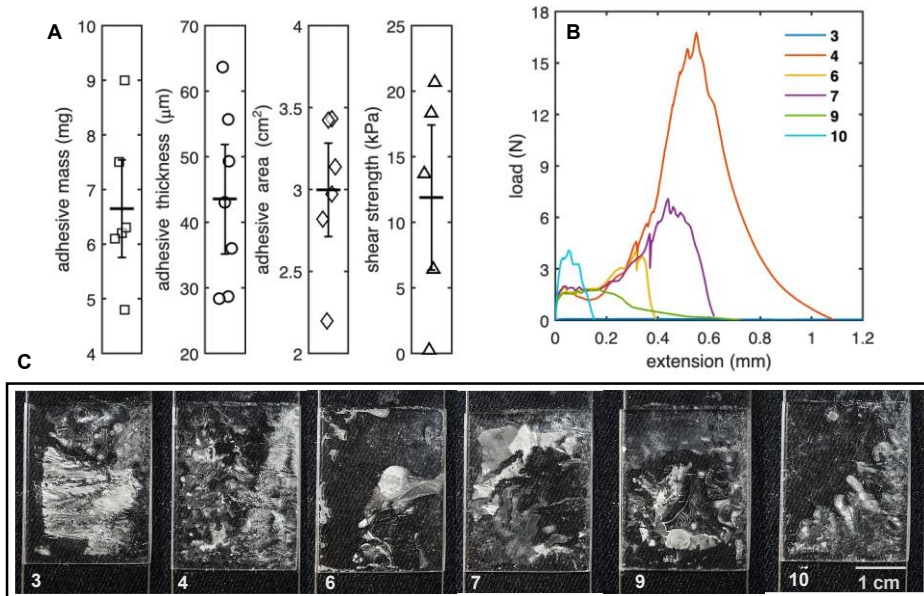


Figure 8. Characterization of smooth glass assemblies bonded with phthalaldehyde via the solvent-assisted bonding method (DCM). **A)** Distributions of adhesive mass, thickness, area, and shear strength, where the average of each is represented as a solid black marker. Error bars represent 95% confidence interval. **B)** Load-extension curves from shear testing. **C)** Optical images of assemblies prior to shear testing. Sample numbers are used to distinguish assemblies within one group.

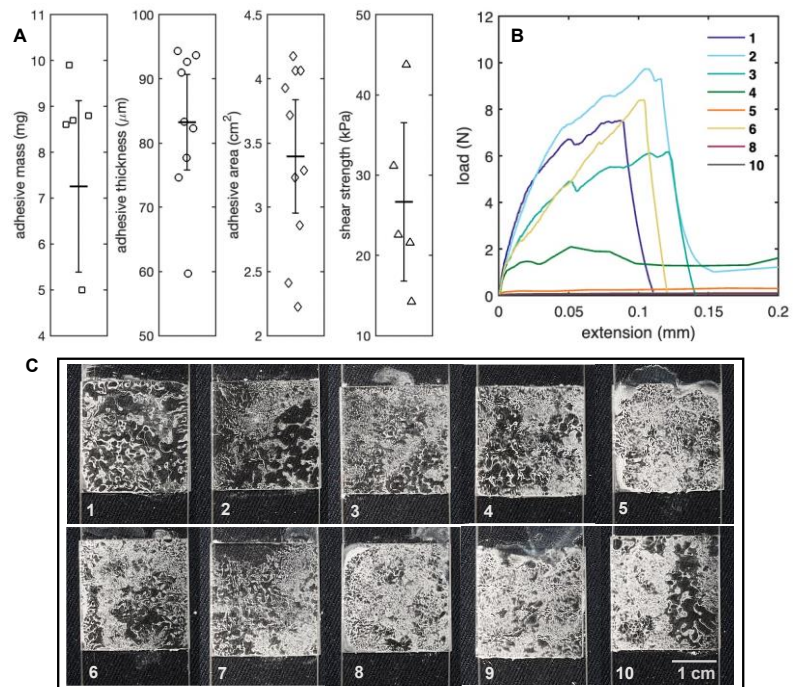


Figure 9. Characterization of smooth glass assemblies bonded with TBS-PPA-TBS (10 kDa) via the solvent-assisted bonding method (DCM). **A**) Distributions of adhesive mass, thickness, area, and shear strength, where the average of each is represented as a solid black marker. Error bars represent 95% confidence interval. **B**) Load-extension curves from shear testing. **C**) Optical images of assemblies prior to shear testing. Sample numbers are used to distinguish assemblies within one group.

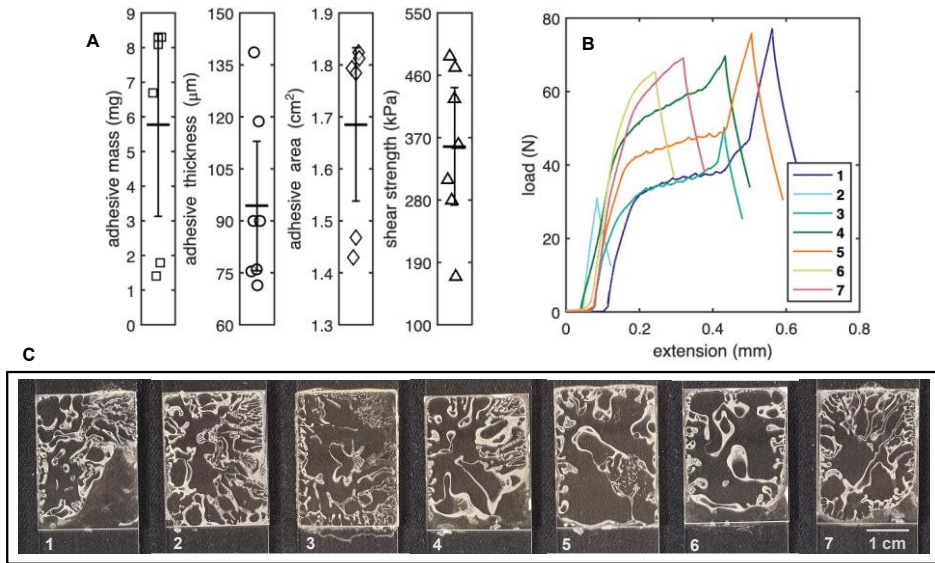


Figure 10. Characterization of smooth glass assemblies bonded with IPA-PPA-Ac (10 kDa) via the solvent-assisted bonding method (DCM). **A)** Distributions of adhesive mass, thickness, area, and shear strength, where the average of each is represented as a solid black marker. Error bars represent 95% confidence interval. **B)** Load-extension curves from shear testing. **C)** Optical images of assemblies prior to shear testing. Sample numbers are used to distinguish assemblies within one group.

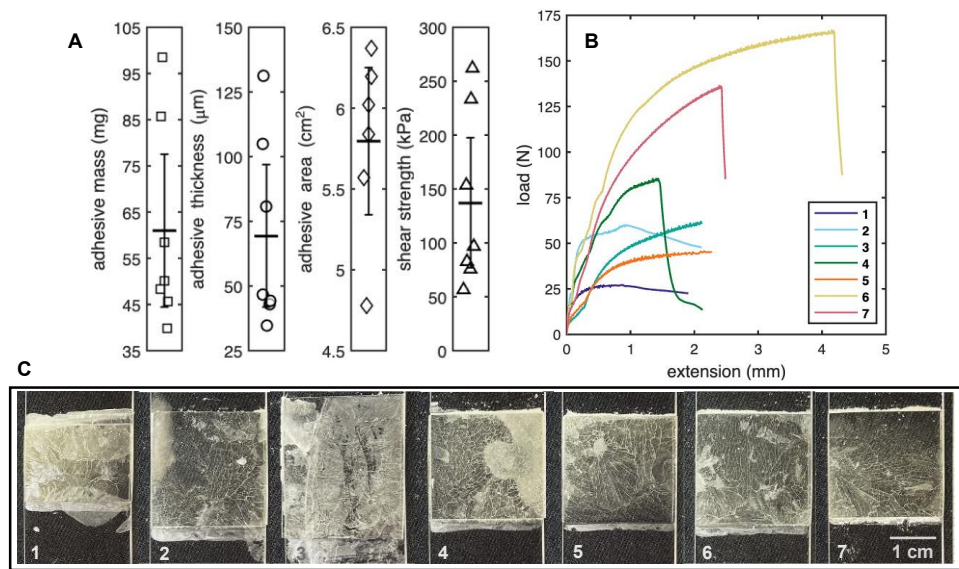


Figure 11. Characterization of smooth glass assemblies bonded with phthalaldehyde via melt bonding. **A)** Distributions of adhesive mass, thickness, area, and shear strength, where the average of each is represented as a solid black marker. Error bars represent 95% confidence interval. **B)** Load-extension curves from shear testing. **C)** Optical images of assemblies prior to shear testing. Sample numbers are used to distinguish assemblies within one group.

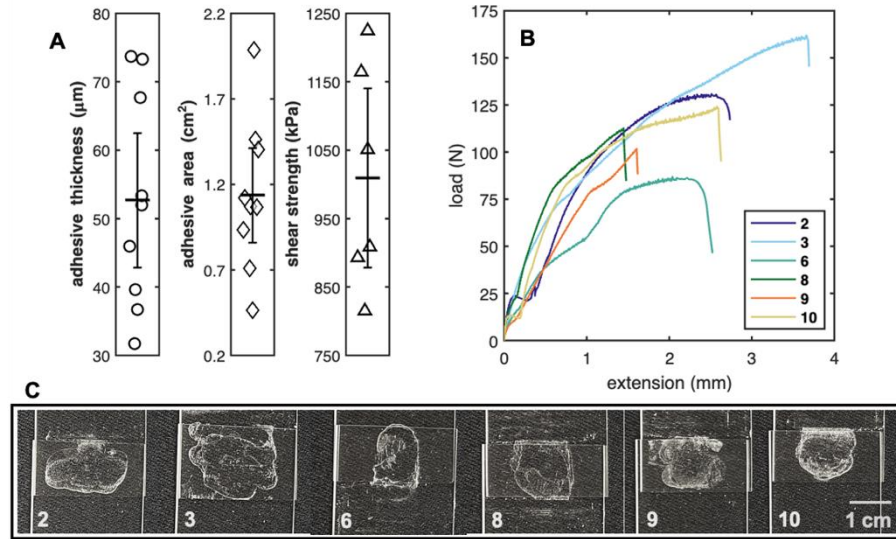


Figure 12. Characterization of smooth glass assemblies bonded with TBS-PPA-TBS (10 kDa) + 20% (w/w) DMP via melt bonding. **A)** Distributions of adhesive mass, thickness, area, and shear strength, where the average of each is represented as a solid black marker. Error bars represent 95% confidence interval. **B)** Load-extension curves from shear testing. **C)** Optical images of assemblies prior to shear testing. Sample numbers are used to distinguish assemblies within one group.

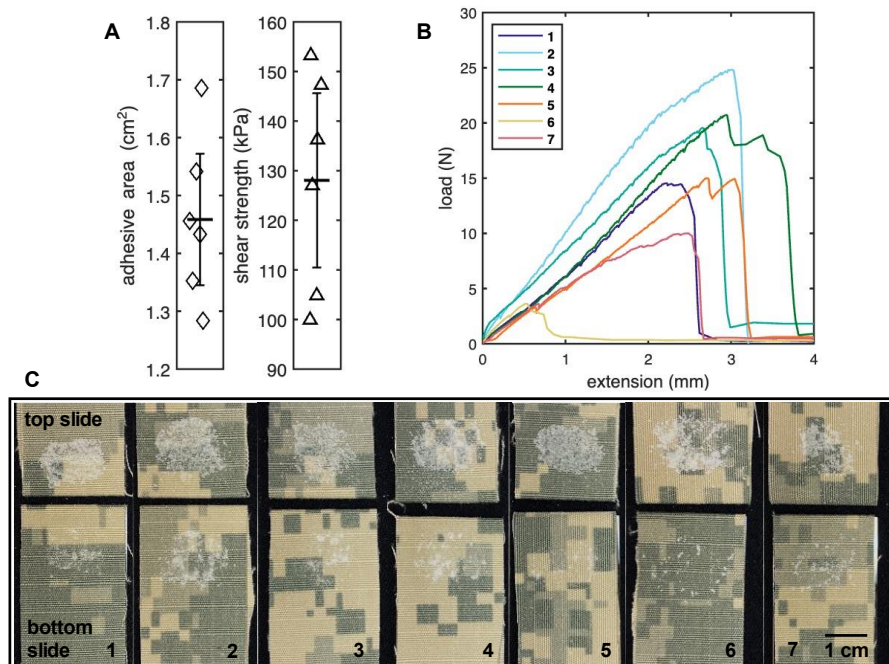


Figure 13. Characterization of rigid NYCO assemblies bonded with TBS-PPA-TBS (10 kDa) + 20% (w/w) DMP via melt bonding. **A)** Distributions of adhesive mass, thickness, area, and shear strength, where the average of each is represented as a solid black marker. Error bars represent 95% confidence interval. **B)** Load-extension curves from shear testing. **C)** Optical images of assemblies prior to shear testing. Sample numbers are used to distinguish assemblies within one group.

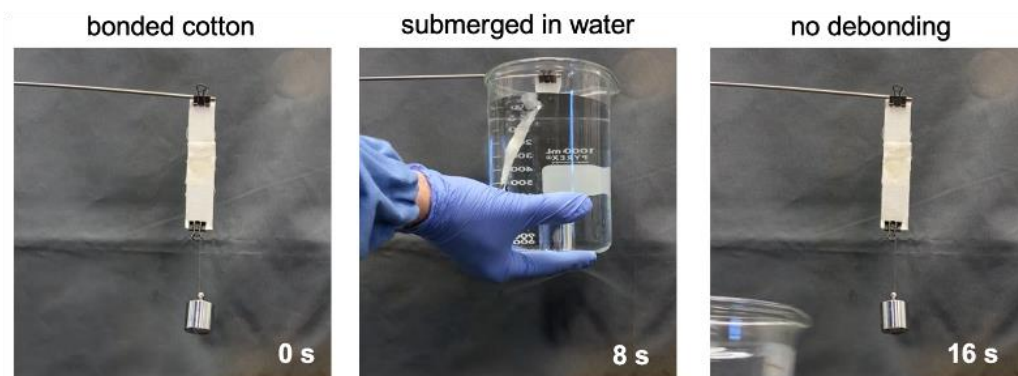


Figure 14. Adhesive performance of cotton substrates bonded with IPA-PPA-Ac after submerging in water. Cotton substrates were bonded with IPA-PPA-Ac ($M_n = 178$ kDa; 50-60 mg of material) via the solvent-assisted bonding method (acetone). No debonding was observed after the bonded assembly was briefly submerged in room temperature water.

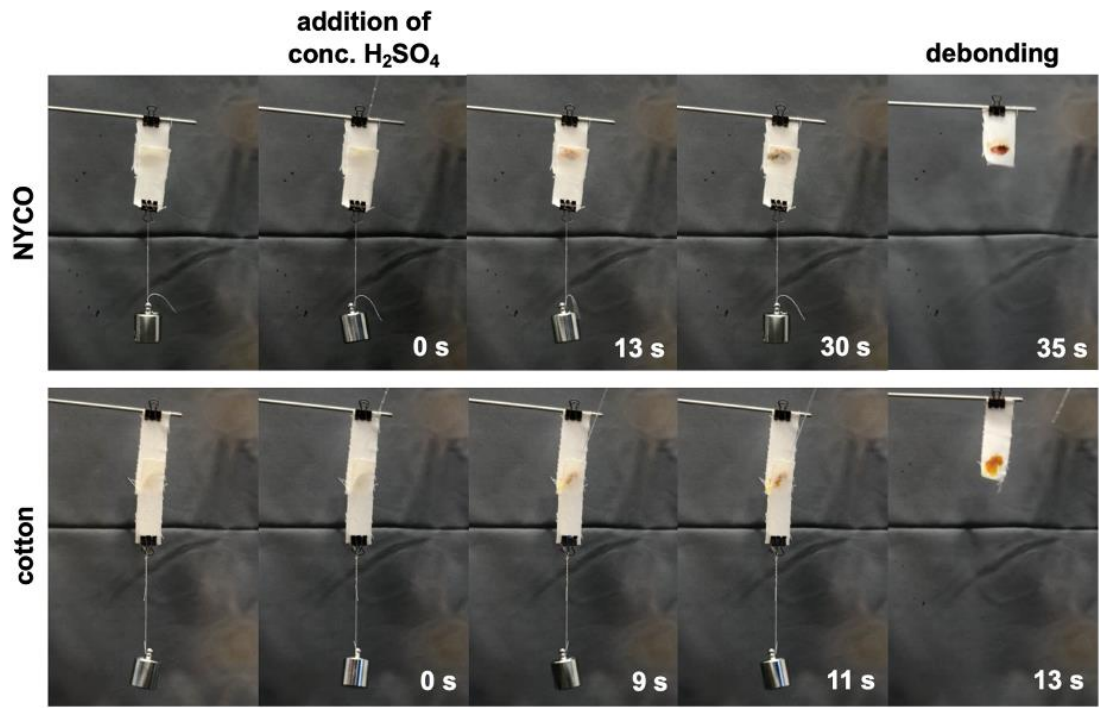


Figure 15. Debonding of cotton and NYCO substrates bonded with IPA-PPA-Ac following exposure to concentrated sulfuric acid. Cotton and NYCO substrates were bonded with IPA-PPA-Ac ($M_n = 178$ kDa; 50-60 mg of material) via the solvent-assisted bonding method (acetone). While the concentrated sulfuric acid led to debonding of both bonded assemblies, delamination occurred in approximately 30 seconds for the NYCO sample and 11 seconds for the cotton sample.

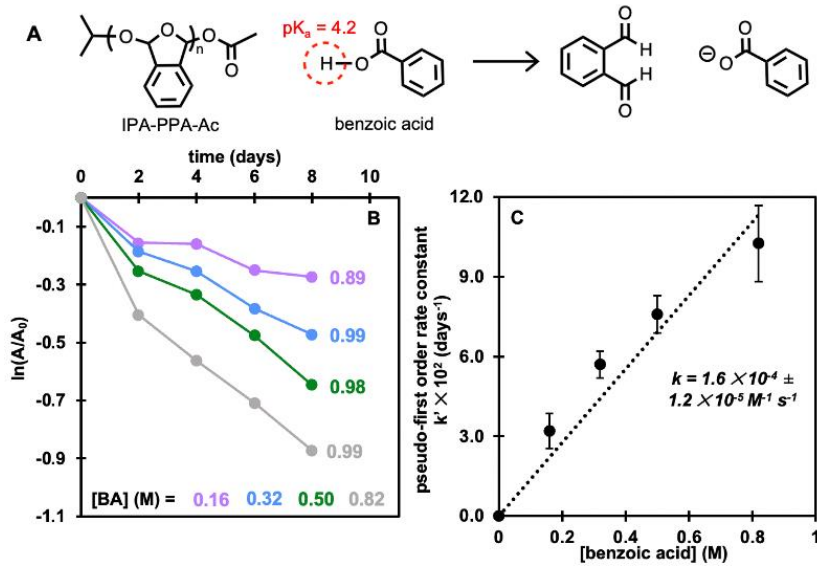


Figure 16. Time-dependent depolymerization of 5.3 mM IPA-PPA-Ac in THF solutions in response to various benzoic acid concentrations (0.16 M in purple, 0.32 M in blue, 0.50 M in green, and 0.82 M in grey). **A)** Depolymerization of PPA in response to benzoic acid. **B)** First order plot tracking PPA depolymerization over 8 days. R^2 values indicated by number adjacent to curves. **C)** Relationship between the pseudo-first order rate constant k' and benzoic acid concentration.

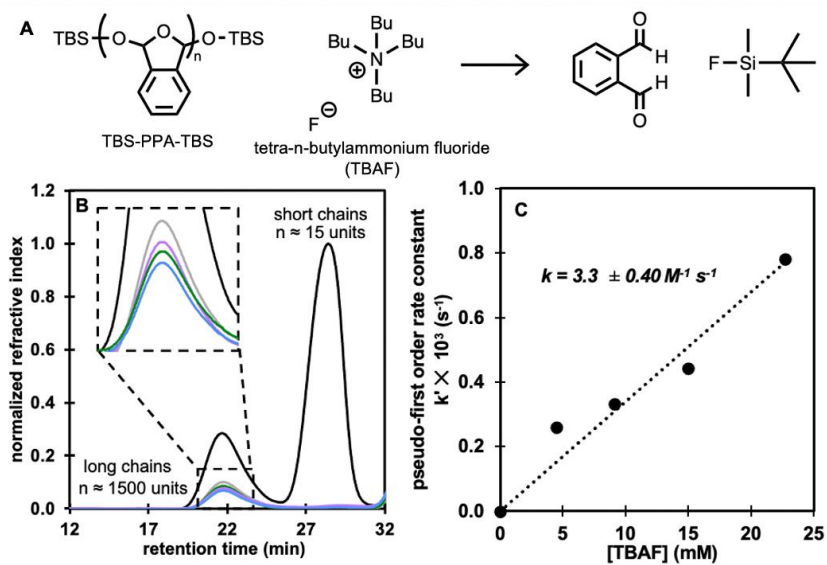


Figure 17. Depolymerization of TBS-PPA-TBS in THF solutions (8.0 mM) in response to various TBAF concentrations. **A)** Depolymerization of PPA in response to TBAF. **B)** GPC traces of control (black) and solutions exposed to TBAF (4.5 mM in grey, 9.1 mM in green, 15.0 mM in purple, and 22.0 mM in blue). **C)** Relationship between the pseudo-first order rate constant k' and TBAF concentration.

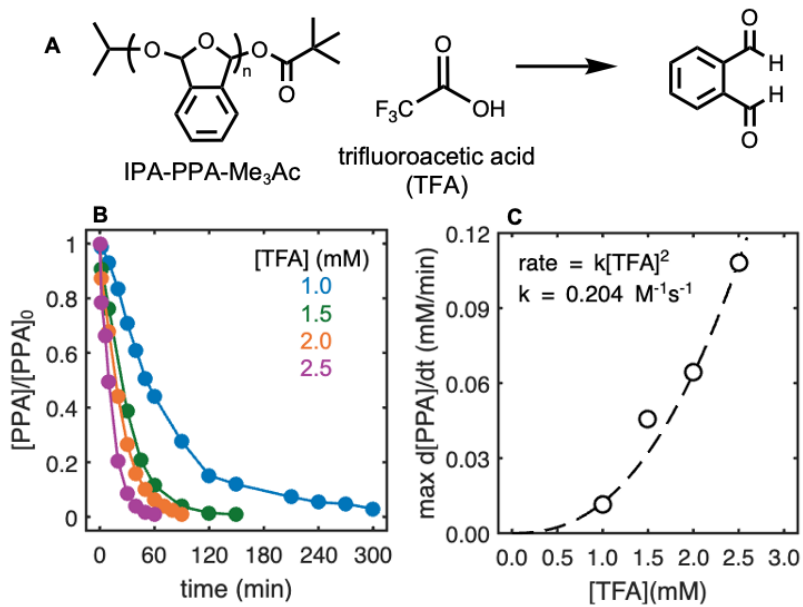


Figure 18. Kinetic analysis of IPA-PPA-Me₃Ac ($M_n = 6.9$ kDa) depolymerization tracked with ¹H-NMR in CD₂Cl₂. **A)** Depolymerization of PPA in response to TFA. **B)** Normalized polymer concentration plotted against time for reactions when the initial polymer concentration is held constant. **C)** Maximum reaction rate plotted against initial TFA concentration. Data fit to inset equation to calculate rate constant.

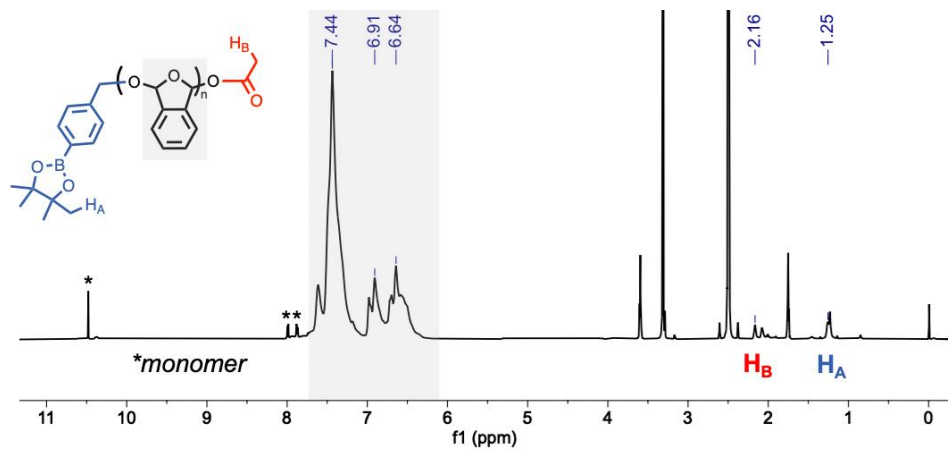


Figure 19. ¹H-NMR spectra (16 scans) of purified Bpin-PPA-Ac (M_n = 28.0 kDa) in DMSO-d₆. Peaks denoted with asterisk represent residual phthalaldehyde monomer.

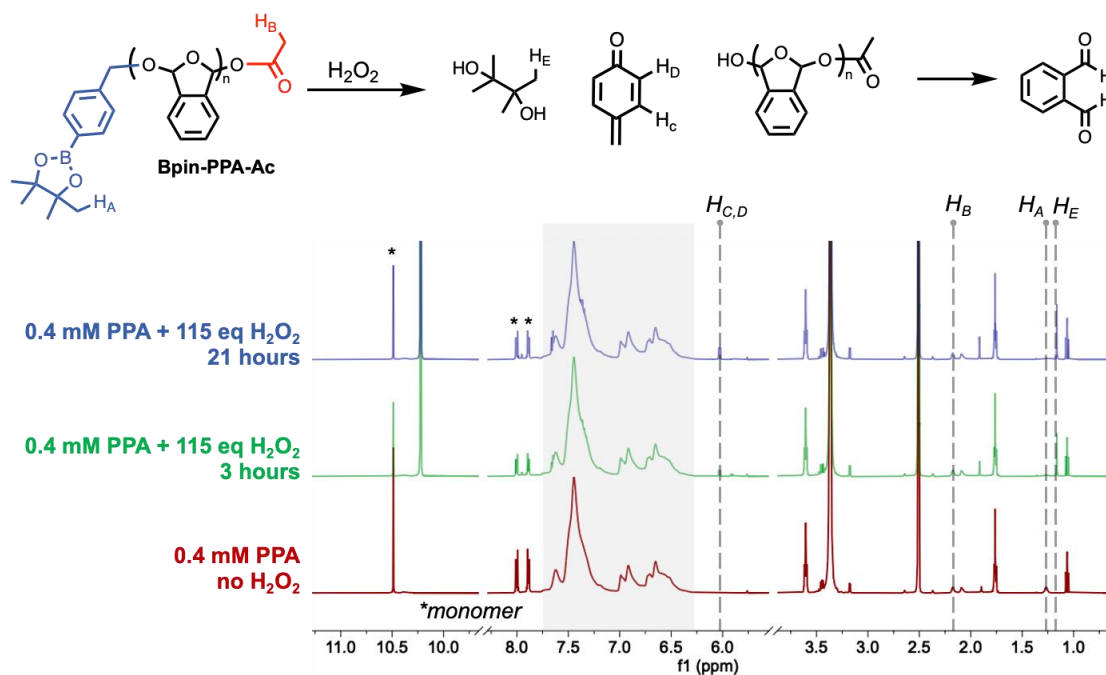
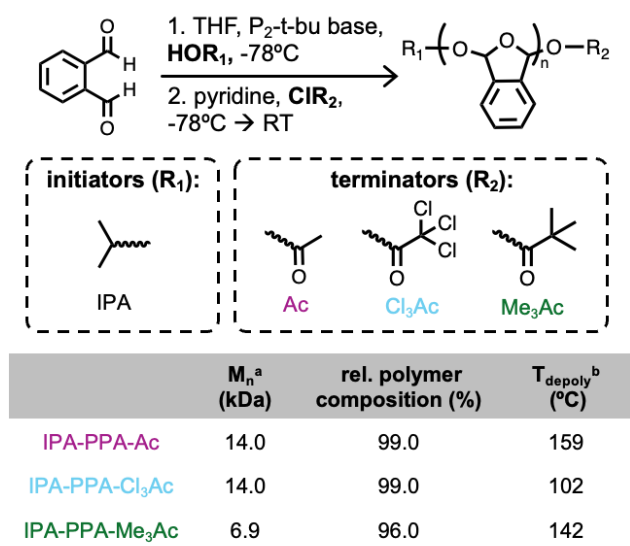


Figure 20. Triggering depolymerization of Bpin-PPA-Ac ($M_n = 28.0$ kDa, DMSO- d_6) with 115 equivalents of hydrogen peroxide (H_2O_2) after 3 hours (green) and 21 hours (blue). No significant depolymerization was observed after treatment with H_2O_2 . Peaks emerge corresponding to protons (H_C , H_D , and H_E) in products formed from end cap cleavage, suggesting the Bpin end cap was cleaved but failed to reveal the reactive polymer terminal.



^acalculated with ¹H-NMR; ^bDSC peak temperature

Figure 21. Synthesis and characterization of linear poly(phthalaldehyde) (PPA). Relative composition calculated from integration of monomer and polymer peaks in ¹H-NMR spectrum.

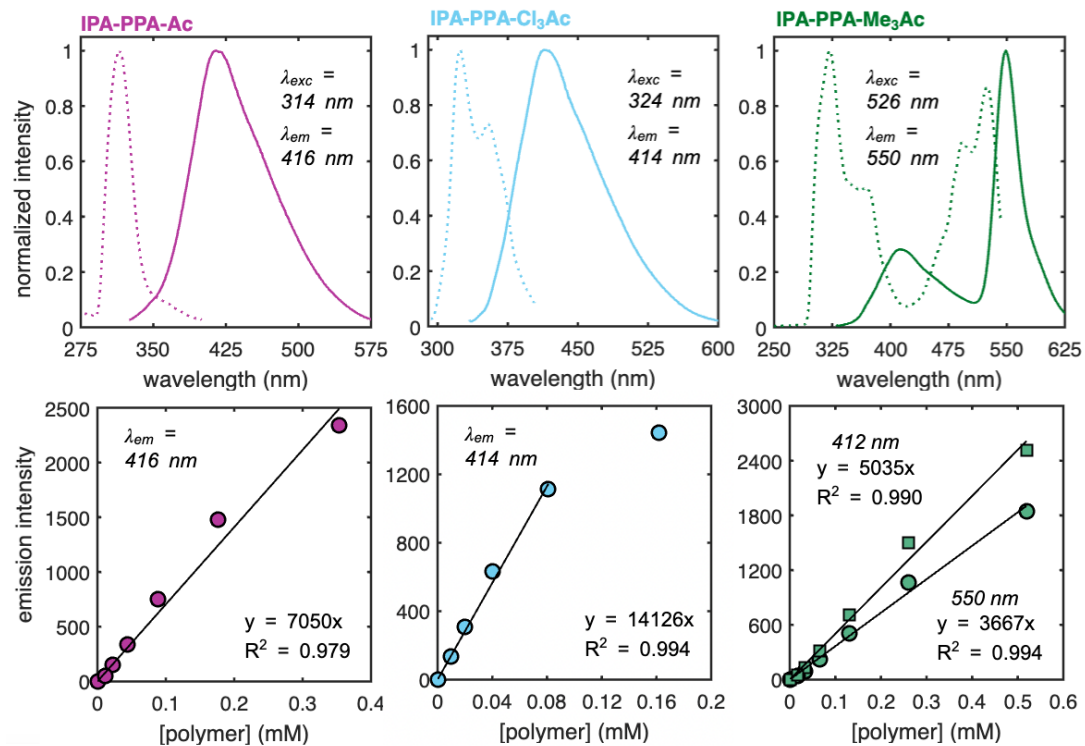


Figure 22. Photoluminescence characterization of DCM solutions of IPA-PPA-Ac ($M_n = 14.0$ kDa, magenta), IPA-PPA-Cl₃Ac ($M_n = 14.0$ kDa, blue), and IPA-PPA-Me₃Ac ($M_n = 6.9$ kDa, green). Normalized excitation (dotted line) and emission (solid line) spectra.

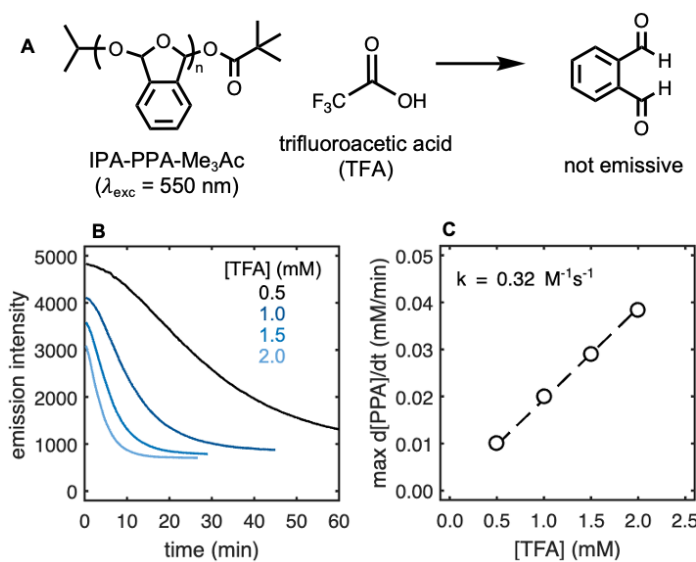


Figure 23. Kinetic analysis of IPA-PPA-Me₃Ac ($M_n = 6.9 \text{ kDa}$, 0.5 mM in DCM) depolymerization tracked with fluorometry ($\lambda_{\text{exc}} = 550 \text{ nm}$). **A)** Depolymerization of PPA in response to TFA. **B)** Normalized polymer emission plotted against time for reactions when the initial polymer concentration is held constant. **C)** Maximum reaction rate plotted against initial TFA concentration. Emission intensity was converted to concentration with a standard curve.



Figure 24. Images of IPA-PPA-Me₃Ac as a glassy solid and in solution (3.5 mM in THF) under a UV lamp ($\lambda_{\text{exc}} = 365 \text{ nm}$).

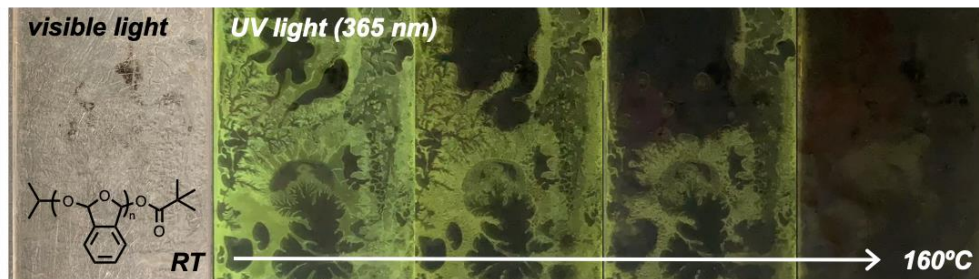


Figure 25. Images of IPA-PPA-Me₃Ac at room temperature under visible light being heated to 160°C under a UV lamp ($\lambda_{\text{exc}} = 365 \text{ nm}$). This polymer depolymerizes around 140°C.

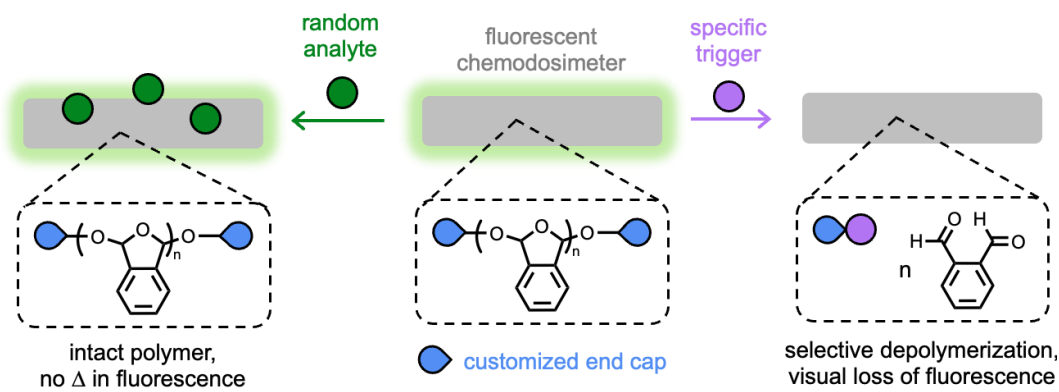


Figure 26. Poly(phthalaldehyde) as a fluorescence chemidosimeter for rapid, selective detection of targeted analytes.

4) Key Outcomes or Other Achievements:

Key outcomes of this work include 3 peer-reviewed publication, 2 manuscripts in preparation, and 1 Master's thesis:

1. Blelloch, N. D., Mitchell, H. T., Tymm, C. C., Van Citters, D. W., and Mirica, K. A.* "Crystal Engineering of Molecular Solids as Temporary Adhesives" *Chem. Mater.* **2020**, *32*, 9882–9896.
2. Blelloch, N. D., Mitchell, H. T., Greenburg, L. C., Van Citters, D. W., and Mirica, K. A.* "Photochemical Control of the Mechanical and Adhesive Properties of Crystalline Molecular Solids" *Cryst. Growth Des.*, **2021**, *21*, 6143-6154.
3. Blelloch, N. D., Yarbrough, H. J., and Mirica, K. A.* "Stimuli-Responsive Temporary Adhesives: Enabling Debonding On-Demand Through Strategic Molecular Design" *Chem. Sci.*, **2021**, *12*, 15183-15205.
4. Yarbrough, H. J., Blelloch, N. D., Van Citters, D. W., and Mirica, K. A.* "Self-Immolative Poly(phthalaldehyde)–Plasticizer Blends: Robust Adhesion and Tunable Debonding Response" *Manuscript in preparation*.
5. Yarbrough, H. J. and Mirica, K. A.* "Intrinsic Fluorescence of Self-Immolative Single Chain Polymer Nanoparticles and its Application in Chemical Sensing" *Manuscript in preparation*.
6. Yarbrough, H. J., "Molecular Engineering of Self-Immolative Polymers as Chemically Responsive Adhesives for Wearable Protection" M.S. Thesis, Dartmouth College, Hanover, NH, 2022.